DOI: 10.53469/wjimt.2026.09(05).04

Facile Fabrication of ZIF-67/Cu_2O for High-Performance Electrochemical CO_2RR to C_2H_4

Xinyu Xu

School of Xi'an Shiyou University, Xi'an 710065, China

Abstract: ***Electrochemical CO_2 reduction (ECO_2RR) offers a sustainable route to convert CO_2 into high-value chemicals, aiding carbon neutrality. Cuprous oxide is a classic catalyst for C_2^+ products, yet it suffers from weak C–C coupling, severe hydrogen evolution side reactions, and low ethylene selectivity at high current densities. Herein, a ZIF-67/Cu_2O composite catalyst was prepared through a facile in-situ growth strategy. Morphological characterization confirms the successful fabrication of a spherical composite with uniform element distribution, abundant active sites and favorable mass transfer pathways. Electrochemical results demonstrate that the introduction of ZIF-67 optimizes the interfacial microenvironment, enhances catalytic activity, and effectively suppresses hydrogen evolution. Benefiting from the synergistic effect between ZIF-67 and Cu_2O, the composite delivers greatly improved ethylene selectivity. In a flow electrolyzer, ZIF-67/Cu_2O achieves a C_2H_4 Faradaic efficiency of 40.05% at 800 mA cm^{-2}, which is much higher than that of bare Cu_2O. This study presents a feasible strategy for constructing high-performance Cu-based composite catalysts toward high current density CO_2-to-ethylene conversion.***

Keywords: Electrochemical CO_2 reduction; Composite catalyst; Ethylene; High current density.

1. INTRODUCTION

Electrochemical carbon dioxide reduction reaction (ECO_2RR) represents a promising technology for the resource utilization of CO_2, which can efficiently convert the greenhouse gas CO_2 into high-value-added carbon-based chemicals and fuels. It possesses crucial application value in mitigating the greenhouse effect and facilitating the achievement of carbon neutrality goals [1,2]. At present, researchers have adopted a variety of catalyst design strategies to realize the highly selective conversion of CO_2 into high-value-added multi-carbon (C_2^+) products, such as ethylene (C_2H_4), ethanol (C_2H_5OH), and n-propanol (C_3H_7OH) [3,4]. Copper (Cu)-based catalysts exhibit moderate adsorption strength toward the key intermediate *CO during the CO_2 reduction process, and are recognized as an ideal catalytic system for efficiently catalyzing ECO_2RR to generate C_2^+ products [5-7]. Nevertheless, monocomponent Cu-based catalysts generally suffer from uneven distribution of active sites, difficulty in precise regulation of surface electronic structure, and intense competition from the hydrogen evolution side reaction. These drawbacks readily lead to negative onset potential, high overpotential, as well as unsatisfactory C_2^+ product selectivity and catalytic stability for CO_2 reduction.

Numerous studies have demonstrated that the carbon-carbon (C-C) coupling of the *CO intermediate serves as the critical step for C_2^+ product formation, which is strongly dependent on the local coverage of adsorbed *CO intermediates [8,9]. Increasing the local *CO coverage can effectively promote C-C coupling. Accordingly, researchers have developed strategies including morphological and size engineering of catalysts [10-13], surface modification [14], and alloying [15] to elevate the local concentration of *CO intermediates and boost the generation of C_2^+ products. Catalyst surface modification enables the precise regulation of ECO_2RR selectivity by modulating the electronic structure, steric hindrance and local microenvironment of catalysts. The modified ligands can alter the adsorption strength of key intermediates (e.g., *COOH, *CO) through electronic effects, thereby steering the reaction pathway toward target products.

The local microenvironment of Cu surfaces, encompassing surface stress, defects, and coordination structures, exerts a decisive influence on the generation of *CO intermediates and subsequent C−C coupling reactions. For example, surface stress modulation can effectively regulate the electronic structure and geometric morphology of Cu surfaces, which further modulates the adsorption energy of reactants and key intermediates as well as reaction kinetics, and ultimately improves the catalytic efficiency of C_2^+ products. Boron possesses an electron configuration of 2s22p1 with unoccupied electron orbitals, which enables it to accept electrons from Cu sites. This electronic modulation optimizes the local electronic properties of Cu and facilitates the overall ECO_2RR process. Notably, under ampere-level high current densities, both rapid *CO generation and accelerated C−C coupling are

urgently required to sustain the continuous proceeding of the C_2^+ reaction pathway and suppress the competing hydrogen evolution reaction (HER). In this context, the rational design of synergistic dual-active-site catalysts can optimize the adsorption and desorption energy barriers of critical reaction intermediates. Such a structural design relieves the catalytic burden of mono-active sites, guarantees efficient *CO formation and C−C coupling, and further breaks the current density limitation of CO_2 electroreduction toward high-value C_2^+ products.

In this work, a core-shell catalyst with Cu_2O as the inner core and ZIF-67/Cu_2O as the outer shell was fabricated through an in-situ growth strategy. Experimental results reveal that the surface modification of ZIF-67 effectively improves the C_2H_4 selectivity during electrochemical CO_2 reduction reaction (ECO_2RR) under high current density. In a flow electrolyzer using 1 M KOH as the electrolyte, the catalyst delivers a high C_2H_4 Faradaic efficiency of 40.05% at 800 mA cm^{-2}, which is distinctly superior to that of pristine Cu_2O(19.44%).

2. EXPERIMENTAL SECTION

2.1 Chemicals and Materials

Cobalt (II) acetate ($Co(OAc)_2$, 99%), 2-Methylimidazole ($C_4H_6N_2$, 99%), Copper(II) chloride dihydrate($CuCl_2$ $2H_2O$, 97%), Ammonium hydroxide ($NH_3 \cdot H_2O$), Ascorbic acid(AA, 99%), ethanol. All chemicals were used without further purification.

2.2 Synthesis of Bare-Cu_2O

In a typical synthesis of Cu_2O, 25 mL of ultrapure H_2O was added to a 50.0 mL glass bottle. The mixture was ultrasonicated until P123 was fully dissolved to form a clear and transparent solution. Subsequently, 15 mL of $[Cu(NH_3)_4]^{2+}$ complex solution was added. The complex solution was prepared by mixing 8 mL of 0.05 M $CuCl_2$ solution with 7 mL of 0.4 M ammonia solution, with a molar ratio of Cu to NH_3 of 1:7. After thorough stirring, 3.8 mL of 0.6 M ascorbic acid (AA) was added dropwise to initiate the reduction reaction. After reacting for 30 min, the obtained yellow dispersion was centrifuged and washed three times with a mixed solution of ethanol and H_2O at a volume ratio of 1:1. The collected precipitate was dried in a vacuum oven at 60 °C for 12 h to yield the yellow powder sample.

2.3 Synthesis of ZIF-67/Cu_2O

In a typical procedure, 30 mg of bare-Cu_2O powder was dispersed in 30 mL ethanol. Subsequently, ethanol solutions containing 5 mg of $Co(OAc)_2$ and 5 mg of 2-methylimidazole were separately added to the above dispersion. After a 5 min reaction, a dark green dispersion was obtained. The resulting product was centrifuged and washed three times with an ethanol/H_2O mixed solution at a volume ratio of 1:1. The collected precipitate was dried in a vacuum oven at 60 °C for 12 h to obtain the dark green powder sample.

3. RESULTS AND DISCUSSION

Preparation and Structural Characterizations of the Catalytic Electrode. The morphology and microstructure of the as-prepared ZIF-67/Cu_2O composite were first characterized by scanning electron microscopy (SEM) and transmission electron microscopy (TEM). As shown in Figure 1a, the sample exhibits well-defined spherical hierarchical structures with uniform particle sizes of approximately 1 μm. The surface of the spheres displays distinct wrinkled and rough textures, inherited from the typical morphology of the ZIF-67 precursor, which is expected to provide abundant active sites and mass transfer channels for electrocatalytic reactions. The internal structure of the material was further revealed by TEM (Figure 1b). The center of the sphere shows a darker contrast, while the edge regions appear brighter, suggesting a loose, porous, or core-shell-like internal structure, consistent with the rough surface features observed in SEM. Meanwhile, no significant aggregation or fragmentation of the particles was observed, indicating good structural stability and monodispersity of the material during the composite process.

To further investigate the elemental distribution within the catalyst, high-angle annular dark-field scanning transmission electron microscopy (HAADF-STEM) and corresponding energy-dispersive X-ray spectroscopy (EDS) elemental mapping analyses were performed on a single particle. As shown in Figure 1c, the HAADF image of an individual catalyst particle presents a uniform bright contrast without significant variations at the edges, preliminarily indicating no severe elemental segregation or phase separation within the particle. The

corresponding EDS mapping results demonstrate that Cu (yellow), Co (green), and N (red) elements are homogeneously distributed throughout the entire spherical particle, with their distribution ranges highly coinciding with the particle contour. Specifically, the uniform distribution of Co and N elements confirms the integrity of the ZIF-67 framework and the stable presence of nitrogen-containing organic ligands in the composite. Meanwhile, the homogeneous distribution of Cu elements indicates that the Cu_2O component is successfully loaded and highly dispersed in the ZIF-67 matrix, without obvious local enrichment or agglomeration.

The above results collectively confirm the successful synthesis of ZIF-67/Cu_2O composites with intact morphology, stable structure, and uniform elemental distribution. This uniformly composite structure provides an ideal structural basis for optimizing charge transfer, interfacial water structure regulation, and anti-flooding performance during the electrocatalytic process.

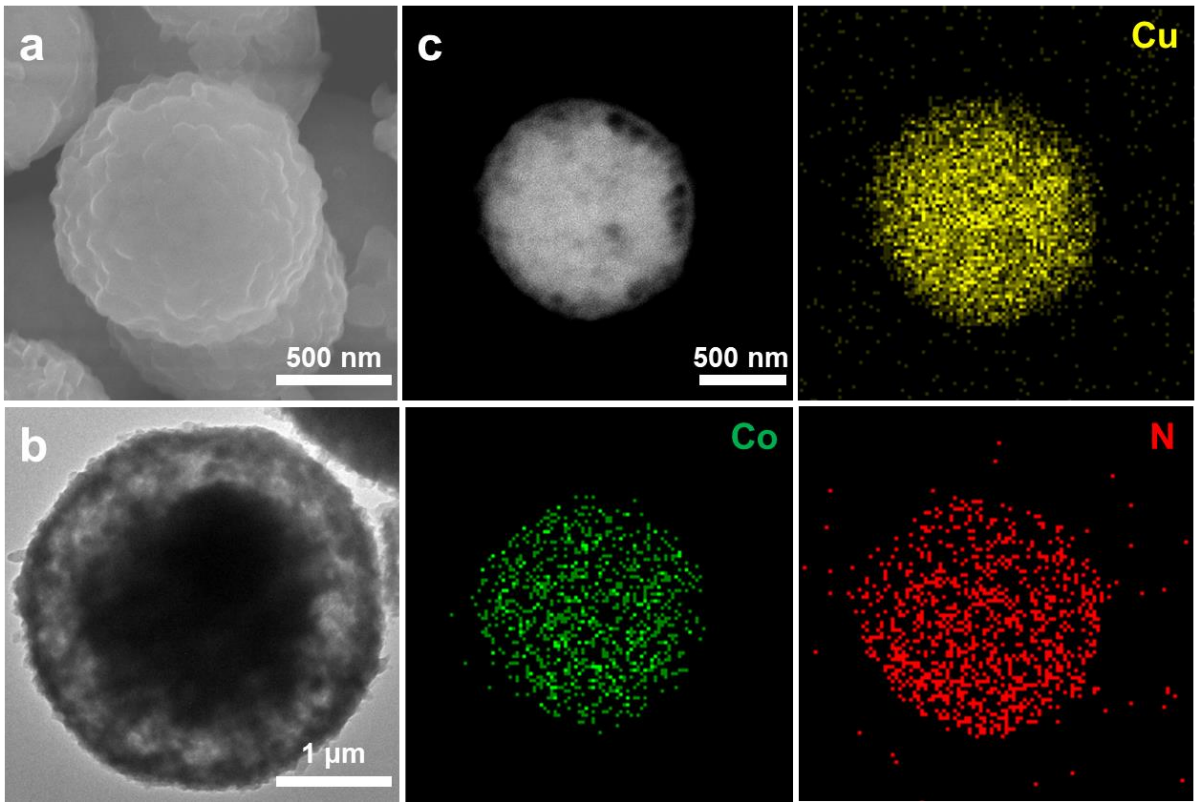

Figure 1: Morphology and elemental distribution of the as-prepared ZIF-67/Cu_2O catalyst. (a) SEM image; (b) TEM image; (c) HAADF-STEM image and corresponding EDS elemental mapping of Cu, Co, and N.

ECO_2RR performance. To evaluate the electrocatalytic CO_2 reduction reaction (ECO_2RR) performance of the as-prepared catalysts, linear sweep voltammetry (LSV) and controlled-current electrolysis tests were conducted.Figure 2a shows the LSV curves of ZIF-67/Cu_2O and None-Cu_2O in CO_2-saturated electrolyte. The ZIF-67/Cu_2O catalyst exhibits a more positive onset potential and higher current density at the same applied potential compared to None- Cu_2O, indicating its enhanced intrinsic activity toward ECO_2RR.

To further investigate the product selectivity, the Faradaic efficiency (FE) of gas products (C_2H_4, CH_4, CO, and H_2) was quantified at various current densities (Figure 2b and 2c). For the None-Cu_2O catalyst (Figure 2b), the FE of C_2H_4 gradually decreases with increasing current density, accompanied by an obvious rise in the FE of the competing hydrogen evolution reaction (HER). In contrast, the ZIF-67/Cu_2O catalyst (Figure 2c) delivers significantly higher C_2H_4 selectivity across the entire tested current density range, with the maximum FE of C_2H_4 reaching over 70% and maintaining high values even at large current densities (up to -1200 mA cm^{-2}). Meanwhile, the FE of H_2 is effectively suppressed on ZIF-67/Cu_2O compared to None- Cu_2O, demonstrating that the introduction of ZIF-67 significantly inhibits HER and promotes C-C coupling for ethylene production.

These results confirm that the ZIF-67/Cu_2O composite not only improves the electrocatalytic activity but also greatly enhances the selectivity and stability toward ethylene in ECO_2RR, which is attributed to the optimized interfacial structure and electronic effect between ZIF-67 and Cu_2O.

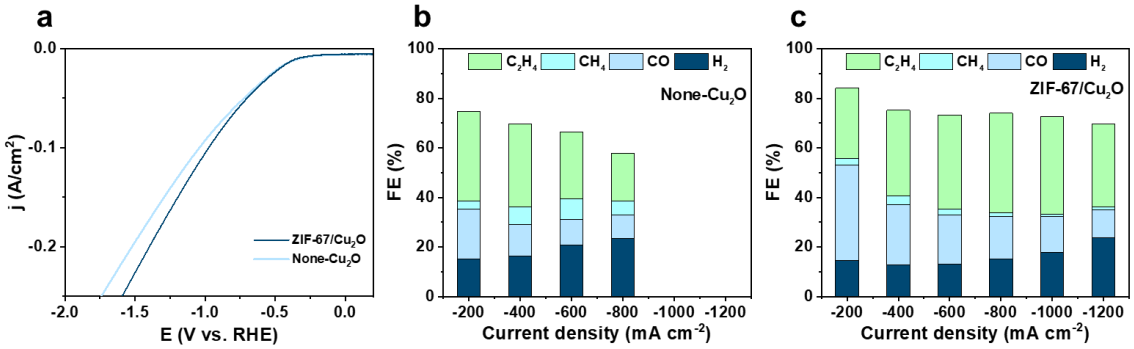

Figure 2: Electrochemical CO_2 reduction performance of ZIF-67/Cu_2O and None- Cu_2O catalysts. (a) Linear sweep voltammetry (LSV) curves recorded in CO_2-saturated electrolyte; Faradaic efficiency (FE) of different products at various current densities for (b) None- Cu_2O and (c) ZIF-67/Cu_2O.

4. CONCLUSIONS

In summary, we have successfully synthesized a ZIF-67/Cu_2O composite catalyst with well-defined spherical morphology, uniform elemental distribution, and excellent electrocatalytic performance for ECO_2RR. Structural characterizations confirm that the Cu_2O component is highly dispersed within the ZIF-67 matrix, forming a stable composite structure that provides abundant active sites and optimized mass transfer pathways. Electrochemical tests demonstrate that the ZIF-67/Cu_2O catalyst exhibits enhanced activity, significantly improved C_2H_4 selectivity, and suppressed HER compared to the None- Cu_2O counterpart, even at high current densities up to -1200 mA cm^{-2}. The superior performance is attributed to the synergistic effect between ZIF-67 and Cu_2O, which modulates the interfacial environment, promotes C-C coupling, and inhibits the hydrogen evolution reaction. This work highlights the rational design of MOF-derived composite catalysts for efficient and selective electrocatalytic CO_2 reduction to ethylene.

REFERENCES

[1] Watkins N B, Schiffer Z J, Lai Y, et al. Hydrodynamics change tafel slopes in electrochemical CO_2 reduction on copper [J]. ACS Energy Letters, 2023, 8: 2185-2192.
[2] Loiudice A, Lobaccaro P, Kamali E A, et al. Tailoring copper nanocrystals towards C_2 products in electrochemical CO_2 reduction [J]. Angewandte Chemie International Edition, 2016, 55(19):5789-5792.
[3] Wu Z Z, Zhang X L, Niu Z Z, et al. Identification of Cu (100)/Cu (111) interfaces as superior active sites for CO dimerization during CO_2 electroreduction [J]. Journal of the American Chemical Society, 2021, 144(1): 259-269.
[4] Hori Y, Kikuchi K, Murata A, et al. Production of methane and ethylene in electrochemical reduction of carbon dioxide at copper electrode in aqueous hydrogencarbonate solution [J]. Chemistry Letters, 1986, 15(6): 897-898.
[5] Zheng Y, Vasileff A, Zhou X, et al. Understanding the roadmap for electrochemical reduction of CO_2 to multi-carbon oxygenates and hydrocarbons on copper-based catalysts [J]. Journal of the American Chemical Society, 2019, 141(19): 7646-7659.
[6] Zhu J, Wang Y, Zhi A, et al. Cation-deficiency-dependent CO_2 electroreduction over copper-based ruddlesden-popper perovskite oxides [J]. Angewandte Chemie International Edition, 2022, 61(3): e202111670.
[7] Liu L X, Cai Y, Du H, et al. Enriching the local concentration of CO intermediates on Cu cavities for the electrocatalytic reduction of CO_2 to C_2^+ products [J]. ACS Applied Materials & Interfaces, 2023, 15(13): 16673-16679.
[8] Zhi X, Jiao Y, Zheng Y, et al. Directing the selectivity of CO_2 electroreduction to target C_2 products via non-metal doping on Cu surfaces [J]. Journal of Materials Chemistry A, 2021, 9(10): 6345-6351.
[9] Kong X, Zhao J, Ke J, et al. Understanding the effect of *CO coverage on C-C coupling toward CO_2 electroreduction [J]. Nano Letters, 2022, 22(9): 3801-3808.
[10] Zhong Y, Kong X, Song Z, et al. Adjusting local CO confinement in porous-shell Ag@Cu catalysts for enhancing C-C coupling toward CO_2 eletroreduction [J]. Nano Letters, 2022, 22(6): 2554-2560.
[11] Reske R, Mistry H, Behafarid F, et al. Particle size effects in the catalytic electroreduction of CO_2 on Cu nanoparticles [J]. Journal of the American Chemical Society, 2014, 136(19): 6978-6986.

[12] Sun B, Dai M, Cai S, et al. Challenges and strategies towards copper-based catalysts for enhanced electrochemical CO_2 reduction to multi-carbon products [J]. Fuel, 2023, 332: 126114.
[13] Ma M, Djanashvili K, Smith W A. Controllable hydrocarbon formation from the electrochemical reduction of CO_2 over Cu nanowire arrays [J]. Angewandte Chemie International Edition, 2016, 55(23): 6680-6684.
[14] Hoang T T, Ma S, Gold J I, et al. Nanoporous copper films by additive-controlled electrodeposition: CO_2 reduction catalysis [J]. ACS Catalysis, 2017, 7(5): 3313-3321.